Electrochemical nucleophilic synthesis of di-*tert*-butyl-(4-[18F]fluoro-1,2-phenylene)-dicarbonate

Qinggang He[a], **Ying Wang**[b], **Ines Alfeazi**[a], and **Saman Sadeghi**[a,*]

[a]Department of Molecular & Medical Pharmacology, University of California, Los Angeles, CA 90095, United States

[b]Division of Theoretical Chemistry & Biology, School of Biotechnology, KTH Royal Institute of Technology, 106 91 Stockholm, Sweden

Abstract

An electrochemical method with the ability to conduct ^{18}F-fluorination of aromatic molecules through direct nucleophilic fluorination of cationic intermediates is presented in this paper. The reaction was performed on a remote-controlled automatic platform. Nucleophilic electrochemical fluorination of tert-butyloxycarbonyl (Boc) protected catechol, an intermediate model molecule for the positron emission tomography (PET) probe (3,4-dihydroxy-6-[18F]fluoro-L-phenylalanine), was performed. Fluorination was achieved under potentiostatic anodic oxidation in acetonitrile containing $Et_3N \cdot 3HF$ and other supporting electrolytes. Radiofluorination efficiency was influenced by a number of variables, including the concentration of the precursor, concentration of $Et_3N \cdot 3HF$, type of supporting electrolyte, temperature and time, as well as applied potentials. Radiofluorination efficiency of $10.4 \pm 0.6\%$ ($n = 4$) and specific activity of up to 43 GBq/mmol was obtained after 1 h electrolysis of 0.1 M of 4-*tert*-butyl-diboc-catechol in the acetonitrile solution of $Et_3N \cdot 3HF$ (0.033 M) and NBu_4PF_6 (0.05 M). Density functional theory (DFT) was employed to explain the *tert*-butyl functional group facilitation of electrochemical oxidation and subsequent fluorination.

Keywords

PET; Radiochemistry; Electrochemical radiosynthesis; Nucleophilic radiofluorination; Aromatic substitution; DFT simulation

1. Introduction

F-18 labeled radiotracers are the cornerstone of positron emission tomography (PET) imaging. The practical and widely available source of radioactive ^{18}F is [18F]fluoride anion produced by the [18]O (p,n) reaction. [18F]fluoride can only react with molecules bearing a partial positive charge on one of its atoms for nucleophilic fluorination. In particular, ^{18}F labeling of aromatic molecules, which is of interest due to unique *in vivo* metabolic

robustness, has been a challenge to achieve (Tredwell and Gouverneur, 2012). Routine radiolabelling of electron rich aromatic molecules such as 3,4-dihydroxy-6-[^{18}F]fluoro-L-phenylalanine ([^{18}F]DOPA) is still conducted using [^{18}F]F$_2$ as the source of electrophilic fluorine (Firnau et al., 1980; Namavari et al., 1992). However, this route has a number of limitations (low specific activity, low yield and maximum theoretical radiochemical yield of 50%, lack of availability of [^{18}F]F$_2$, downstream purification due to high reactivity of F$_2$), which have limited wider clinical adoption and availability of [^{18}F] DOPA (Guillaume et al., 1991; Lemaire et al., 1994).

Oxidative [^{18}F]fluoride ion transfer has been employed to produce radiotracers with highly fluorophilic Pd and Ni based complexes, enabling radiolabelling with [^{18}F]fluoride (Lee et al., 2011, 2012). An alternative approach to activate aromatic molecules for reactions with fluoride ion is to reduce the electron density at the reaction center. Among the methods to generate an electron-poor carbon in arenes (Ermert et al., 2004; Gao et al., 2012; Nozaki and Tanaka, 1967; Shiue et al., 1984), electrochemical anodic oxidation is technically elegant because the reactions can be carried out under mild conditions and there is no hazardous chemical oxidant required (Fuchigami and Inagi, 2011). Radiofluorination of complex molecules by electrochemistry has been done under galvanostatic conditions by Reischl et al. in their series publications (Kienzle et al., 2005; Reischl et al., 2002, 2003). Different from the umpolung strategy (Gao et al., 2012), the oxidation effect can be precisely controlled by the applied potential on the working electrode. The accurate control is provided by the direct relation of electron density and redox potential for different carbon atoms with various substituents on the benzene ring. In general, aromatic compounds with both electron withdrawing groups and electron donating groups can be electrochemically fluorinated according to a 4-step process (Noel et al., 1997; Reischl et al., 2002; Rozhkov, 1976). The electrochemical fluorination method has several advantages for radiofluorination of aromatic compounds. First, neither pre-activation of aromatic ring by electron withdrawing functional groups (e.g. nitro) nor post-elimination of these groups is required. Secondly, the fluorine source is from the free fluoride ion in the solution and may be used without modification. Thirdly, there is no directing group hindrance or synthetic difficulty in preparing precursors. Finally, the delicate control of oxidation potential makes highly regioselective radiofluorination feasible (Fuchigami and Inagi, 2011; Noel et al., 1997).

In this paper, electrochemical nucleophilic synthesis of di-*tert*-butyl-(4-[^{18}F]fluoro-1,2-phenylene)-dicarbonate **5** was conducted under potentiostatic conditions. The function and effect of *tert*-butyl leaving group for fluorination of aromatics was examined with a computational study using density functional theory. Di-*tert*-butyl-(4-(*tert*-butyl)-1,2-phenylene)-dicarbonate **6** was synthesized and electrochemical radiofluorination of the above precursor was conducted on a specifically developed automated electrochemistry platform. This compound is a relevant model to an important class of PET radiopharmaceuticals and can potentially be converted to [^{18}F]DOPA (Kaneko et al., 1999). The products were detected and identified with mass spectrometry (MS), high-performance liquid chromatography (HPLC) and thin layer chromatography (TLC). Several variables, such as the concentrations of the precursor and the electrolyte, the effect of the supporting

electrolyte, reaction temperature, and applied potentials were studied to achieve the optimum radiochemical yield.

2. Experimental

2.1. Theoretical studies

All density functional theory (DFT) calculations were carried out with the Jaguar 7.6 program package by Schrödinger LLC. For geometry optimizations, solvation energy, and frequency calculations, Becke's three-parameter hybrid functional and the LYP correlation functional (B3LYP) (Becke, 1993; Lee et al., 1988) was used with the 6-311$G^{**}++$ basis set. Frequency calculations were performed on the optimized geometries to verify that the geometries correspond to minima on the potential energy surface (PES). The Gibbs free energies were defined as the following equation $G = E$ (B3LYP/6-311$G^{**}++$) + G_{solv} + ZPE + H_{298}-TS_{298}. The solvation model applied (in acetonitrile) was the Poisson-Bolzmann reactive field implemented in Jaguar 7.6 (PBF) (Marten et al., 1996). All potential values were given vs. NHE (normal hydrogen electrode).

2.2. Chemicals

HPLC grade acetonitrile (MeCN) was purchased from Fisher Scientific and distilled over CaH_2 to prepare the anhydrous solvent. Triethylamine trihydrofluoride ($Et_3N \cdot 3HF$), tetrabutylammonium perchlorate (NBu_4ClO_4) and tetrabutylammonium hexafluorophosphate (NBu_4PF_6) were ordered from Sigma-Aldrich and used as received.

2.3. Synthesis of the "cold" organic compounds

To conduct radiofluorination of catechol, Boc protection was used to protect the hydroxyl function on the aromatic ring. 4-(*tert*-butyl)benzene-1,2-diol (3.0 g, 0.018 mol) was dissolved in 20 mL of anhydrous dichloromethane. The solution was cooled down in an ice bath. Triethylamine (21.8 g, 0.216 mol) was added drop wise to the cooled solution. After completion of the addition, 1,2-pheny-lene-di-*tert*-butyl-dicarbonate (15.4 mL, 0.072 mol) was added drop wise to the resulting solution. The reaction mixture was then stirred at room temperature overnight. The reaction was quenched with 100 mL of water. The aqueous layer was extracted with dichloromethane (3×50 mL) after layer separation. The organic phase was then washed with brine (100 mL), dried over sodium sulfate and evaporated to dryness. The residue was recrystallized from hexane and dried in vacuum, yielding 5.85 g (85%) of compound **6** in the form of white crystals. The melting point of compound 6 measured by an "Electrochemical Melting Pointing" apparatus was 80–82 °C. A Bruker AV 600 NMR instrument and a Thermo Fisher Scientific Exactive Plus mass spectrometer were used for characterization of the compounds. ^{1}HNMR (CDCl$_3$): δ = 1.29 (s, 9H, C (CH$_3$)$_3$), 1.53 (s, 9H, Boc), 1.54 (s, 9H, Boc), 7.14 (d, 1H, 6-H), 7.17 (d, 1H, 5-H), 7.21 (s, 1H, 3-H). MS (DART, *m/z*): 367.21074 (M + H$^+$).

Compound **5** (77%, melting point: 97–99 °C) was synthesized according to the above procedure starting from 4-fluorobenzene-1,2-diol. ^{1}HNMR (CDCl$_3$): δ = 1.53 (d, 18H, Boc), 6.89–6.95 (m, 1H, 3-H), 7.02 (dd, 1H, 4-H), 7.19 (dd, 1H, 6-H). ^{19}FNMR (CDCl$_3$): δ = 114.11. MS (DART, *m/z*): 329.13905 (M + H$^+$).

Compound **10** (di-*tert*-butyl-(3-fluoro-1,2-phenylene)-dicarbonate, 81%, melting point: 90–92 °C) was synthesized according to the above procedure starting from 3-fluorobenzene-1,2-diol. ^{1}HNMR (CDCl$_3$):1.56 (s, 18H, Boc), 6.92–7.00 (ddd, 1H, 5-H), 7.04–7.09 (dd, 1H, 6-H), 7.20-7.26 (dd, 1H, 3-H). ^{19}FNMR (CDCl$_3$): δ = −126.65. MS (DART, *m/z*): 329.13888 (M + H$^+$).

2.4. Electrochemical experiments

Electrochemical radiofluorination was conducted in a three-electrode system under a constant – potential mode controlled by an Autolab128 potentiostat-galvanostat (Metrohm USA). All electrochemical experiments were conducted in a cylindroid glass beaker cell with a total volume of 20 mL During the experiments 6 mL of electrolyte was loaded. Two Pt mesh electrodes were used as the working (5.23 cm^2) and the counter (6.65 cm^2) electrodes. A leakless Ag/AgCl electrode (EDAQ Inc, USA) was used as the reference electrode.

The undivided cell was combined with a [^{18}F]fluoride ion delivery line. [^{18}F]fluoride was originally generated in 0.5 mL of [^{18}O]water from the cyclotron. The radioactivity was trapped on a MP-1$^®$ anion exchange resin by passing the above solution through. Majority of the water on the resin was removed by washing with 10 mL of anhydrous MeCN and drying with ultra-pure Ar for 5 min. Then [^{18}F]fluoride was eluted out from the column with Et$_3$N · 3HF in different concentrations.

A pulsing technique, switching the potential from a high level to a low level periodically, was used to minimize the surface polymerization and poisoning issues. In this work, all electrolysis products were analyzed after 38 cycles of pulsing between 2.7 V (90 s) and 0.4 V (5 s).

2.5. Characterization methods

Analytical HPLC for product identification was conducted using a Knauer K-501 HPLC pump, coupled with a Knauer K-2500 UV detector (254 nm) and a NaI (Tl) scintillation detector. A Gemini$^®$ HPLC column (150 × 4.6 mm^2, 5μ) C18 column was used and eluted with MeOH/H$_2$O (70/30; v/v) at a flow rate of 2.1 mL min^{-1}. To analyze the regioselectivity of the reaction, MeOH/H$_2$O (60/40; v/v) at a flow rate of 2.0 mL min^{-1} was used for clear separation of di-*tert*-butyl-(4-fluoro-1,2-phenylene)-dicarbonate **5** and di-*tert*-butyl-(3-fluoro-1,2-phenylene)-dicarbonate **10** (Fig. 7).

In order to make accurate calculation for the radiofluorination efficiency, TLC measurements were performed on an AR-2000 TLC Imaging Scanner (Bioscan, Washington DC, USA) using dichlormethane as the single mobile phase.

To purify the products of the reaction, water (30 mL) was added to the electrolyte solution and the mixture was passed through a Sep-Pak$^®$ C18 Classic Cartridge. Subsequently the product was eluted by 3 mL of methanol.

3. Results and discussion

3.1. Structural modification of the substrate of catechol

It has been reported that ^{18}F-labeled catechol can potentially be converted to ^{18}F-DOPA (Kaneko et al., 1999). However, synthesis of ^{18}F-catechol via electrochemical fluorination of catechol is challenging. In our experiments, the hydroxyl function on the aromatic ring was easily oxidized at 0.55 V (vs. Ag/AgCl). More specifically, electrons will be drawn from hydroxyl groups at much lower potentials than the aromatic rings. A few common protecting groups such as acetyl, *tert*-butyloxycarbonyl, methoxymethyl ether, etc. were screened during this study. The *tert*-butyloxycarbonyl (Boc) protected compound showed stability and the highest radiofluorination efficiency. Further studies reported here were performed on Boc protected compounds.

[18F]Fluoride to enhance regioselectivity of fluorination of catechol, some insight into the mechanistic study is provided by the effect of the *tert*-butyl as the leaving group (Fig. 1). For **1**, where there is no *tert*-butyl substitution, the potential of oxidation to form the radical cation **2**, an important and necessary intermediate step for fluorination of the aromatic moiety, calculated to be 2.08 V. A radical **3** is generated after nucleophilic attack by fluoride ion, and a further oxidation to the cation **4**, calculated at 0.99 V. For the *tert*-butyl substituted compound **6**, the potential of first oxidation step is calculated to be only 1.95 V. The value is 130 mV lower due to the stabilization of the resulting cation radical **7** by electron-donating *tert*-butyl group, which indicates that oxidation of the *tert*-butyl substituted complex could proceed at a milder potential. The potential of the second oxidation step is calculated at 0.91 V, which is also slightly lower than that of the former approach (0.99 V).

In our analysis of the orbitals related to oxidation, we calculated the Highest Occupied Molecular Orbital (HOMO) for **1** and **6**, since one electron needs to be removed from the HOMO when oxidation occurs (Fig. 2). The calculated HOMO energy of **6** shows a higher value of −0.249 a.u. compared to the corresponding value for **1**, which is −0.257 a.u. This implies that it is easier for **6** to lose one electron (1.95 V) and complete the oxidation than that for **1** (2.08 V). For the second oxidation step of radicals **3** and **8**, there is only one electron on the HOMO that can be considered as a Singly Occupied Molecular Orbital (SOMO). The SOMO energy of **8** is calculated to be −0.207 a.u. and remains higher than that of **3** (−0.213 a.u.). This indicates that it is easier to remove one electron from **8** than from **3**, which is consistent with the calculated oxidation potentials (0.91 V and 0.99 V for **8** and **3** respectively).

The comparison shows that the electro-donating *tert*-butyl substituent can reduce the oxidation potential of the aromatic substrate significantly while subsequent dissociation following the second oxidation step may be facilitated due to the high stability of *tert*-butyl cation.

3.2. Cyclic voltammetry

Fig. 3 shows the cyclic voltammogram of acetonitrile solution of $Et_3N \cdot 3HF$ (0.05 M) in the absence and presence of precursor **6**. It can be seen that the $Et_3N \cdot 3HF$ electrolyte itself can be oxidized on the Pt working electrode with notable current beyond 0.85 V (vs. Ag/AgCl). However, upon addition of 0.005 M precursor **6**, significant increase of current can be observed with the threshold (onset) of 2.27 V, indicating anodic oxidation and further fluorination of **6**. While an oxidation potential higher than the onset at 2.27 V is required, increasing the potential will increase side products including any decomposition from the oxidation of **5** ($E_{onset} = 2.35$ V). From our screening experiments, the best chemical yield (molar ratio of the fluorinated product and the precursor) was obtained at 2.7 V. As a result, in this work, all electrolysis was performed under a potentiostatic condition of 2.7 V.

3.3. Radiofluorination efficiency

Consumption rate of precursor **6**, chemical yield of **5** (based on the starting concentration of the precursor) and the radiofluorination efficiency results are summarized in Fig. 4 and Table 1. Fig. 4 shows that the consumption rate of the precursor remained rather stable as the concentration of the precursor changed. However, the chemical yield drops linearly as a function of the concentration of the precursor. Considering the formation of a cation radical as the prerequisite of anodic fluorination (Reischl et al., 2002), a plausible explanation is the formation of dimers and/or polymers with increasing ratio of precursor to fluoride (Belding et al., 2008). Using only $Et_3N \cdot 3HF$ as the electrolyte at room T the best radio-fluorination efficiency was $2.7 \pm 0.6\%$. To improve the solution conductivity, supporting electrolytes (NBu_4ClO_4 and NBu_4PF_6) were added and electrolysis was conducted as before. The rows 6 and 7 in Table 1 show the TLC results of electrochemical fluorination of 0.05 M **6** with 0.033 M $Et_3N \cdot 3HF$ in the absence and presence of 0.05 M NBu_4ClO_4, which increased radio-fluorination efficiency by a factor of five.

The instability of the Boc protecting groups in acidic media similar to that used during electrolysis here is documented (Namavari et al., 1992). The unprotected t-Bu-catechol may be oxidized on Pt surface and passivate the electrode surface (see Fig. S1), which has a detrimental effect on radio-fluorination efficiency. Use of other protecting groups, adjusting pH of the reaction mixture or lowering the reaction temperature may alleviate this problem. To partially test this hypothesis, radiofluorination was conducted at 0 °C and the results were compared with those obtained at room temperature. Table 1 shows that the radiofluorination efficiency was nearly doubled by lowering the T from 25 °C to 0 °C. The above results are consistent with those reported in the literature (Kienzle et al., 2005). Additionally, we investigated the effect of the supporting electrolyte by adding NBu_4PF_6 instead of NBu_4ClO_4. Similar to NBu_4ClO_4, NBu_4PF_6 was chosen due to its wide potential window (high stability) during electrolysis. The change resulting from the supporting electrolyte effect was minor and the best radiofluorination efficiency values were obtained using NBu_4PF_6 as the supporting electrolyte with results presented in Fig. 5.

Although the yields (as measured by TLC) are instructive, actual recovered product yields (true radiochemical yields) may be of more general interest from a practical point of view. The product of di-*tert*-butyl-(4-[^{18}F]fluoro-1,2-phenylene)-dicarbonate was purified using

Sep-Pak® C18 classic cartridges. Radiochemical purity was achieved and Fig. 6 illustrates that free [18F]fluoride ions and 18F-labeled side products have been removed efficiently. The decay corrected radiochemical yields for the last entry (row) in Table 1 were $8.9 \pm 1.6\%$ (*n*=3) after 65 min with a synthesis time of 60min and typical purification taking 5 min. These values are fairly close to the radiofluorination efficiency values shown in the last row of Table 1, which indicates minimal loss of the product during purification, with no co-elution of side products. Starting activity ranged from 300 to 600 mCi. Specific activity was calculated for experiments in the last row in Table 1. Specific activity measurement was based on measurement of the decay corrected activity of the final radiochemically pure product and the mass as measured from area under the curve in the UV HPLC trace and the calibration curve prepared from the cold standard. The maximum specific activity value of 43 GBq/mmol achieved in these experiments is comparable to those reached by electrophilic fluorination with [18F]F$_2$ (Namavari et al., 1992; Reischl et al., 2002).

Finally, to exclude the possibility of formation of di-*tert*-butyl-(3-[18F]fluoro-1,2-phenylene)-dicarbonate **10** (Fig. 7) we conducted HPLC with both standard isomers (**5** and **10**) as well as the products after purification. Fig. 7 clearly shows that only di-*tert*-butyl-(4-[18F]fluoro-1,2-phenylene)-dicarbonate **5** with a retention time, 1.3 min later than that of **10**, was formed after electrochemical fluorination of **6**. It confirms the DFT results that the *tert*-butyl leaving group effectively directs the position of fluorination.

4. Conclusion

For the first time, it has been demonstrated that electrochemical nucleophilic synthesis of di-*tert*-butyl-(4-[18F]fluoro-1,2-phenylene)-dicarbonate **5**, under controlled potentiostatic conditions, is feasible. A *tert*-butyl substitution group on the aromatic ring was selected based on computational study of density functional theory. The calculation results imply that a cationic stable electron donating substitution group such as *tert*-butyl can reduce the redox potential of the substrate, resulting in favorable electrochemical fluorination precursors. Different from traditional nucleophilic fluorination through an S$_N$2 substitution, where an electron withdrawing group is often used as the leaving group, *tert*-butyl was effective for electrochemical fluorination to promote a higher product yield. Electrochemical radiofluorination of 4-[18F]fluoro-diboc-catechol was confirmed by HPLC and TLC analysis. The crude product was purified and decay corrected radiochemical yields of $8.9 \pm 1.6\%$ were achieved with 0.1 M of di-*tert*-butyl-(4-(*tert*-butyl)-1,2-phenylene)-dicarbonate in acetonitrile containing 0.033 M Et$_3$N · 3HF and 0.05 M NBu$_4$PF$_6$ after 1 h of electrolysis at 0 °C on a custom built automatic platform. The maximum specific activity value of 43 GBq/mmol is comparable to those reached by electrophilic fluorination with [18F]F$_2$. Variables such as water content, the type and the concentration of the electrolyte, modification of cell geometry and incorporation of flow-through synthesizers (Sadeghi et al., 2013), can potentially be optimized to obtain higher radiochemical yields. All experiments in this paper were carrier-added with Et$_3$N · 3HF as the fluoride source. Achievement of region-specific electrochemical nucleophilic radiofluorination of aromatic moieties in a carrier-free system should further expand the applicability of the method presented here and enable production of PET probes with high specific activity.

Supplementary Material

Refer to Web version on PubMed Central for supplementary material.

Acknowledgment

References

Becke AD. Density-functional thermochemistry. III. The role of exact exchange. J. Chem. Phys. 1993; 98:5648–5652.

Belding SR, Rees NV, Aldous L, Hardacre C, Compton RG. Behavior of the heterogeneous electron-transfer rate constants of arenes and substituted anthracenes in room-temperature ionic liquids. J. Phys. Chem. C. 2008; 112:1650–1657.

Ermert J, Hocke C, Ludwig T, Gail R, Coenen HH. Comparison of pathways to the versatile synthon of no-carrier-added 1-bromo-4-[18F]fluorobenzene. J. Label. Compd. Radiopharm. 2004; 47:429–441.

Firnau G, Chirakal R, Sood S, Garnett S. Aromatic fluorination of xenon difluoride: l-3,4-dihydroxy-6-fluoro-phenylalanine. Can. J. Chem. 1980; 58:1449–1450.

Fuchigami T, Inagi S. Selective electrochemical fluorination of organic molecules and macromolecules in ionic liquids. Chem. Commun. 2011; 47:10211–10223.

Gao Z, Lim YH, Tredwell M, Li L, Verhoog S, Hopkinson M, Kaluza W, Collier TL, Passchier J, Huiban M, Gouverneur V. Metal-free oxidative fluorination of phenols with [18F]fluoride. Angew. Chem. Int. Ed. 2012; 51:6733–6737.

Guillaume M, Luxen A, Nebeling B, Argentini M, Clark JC, Pike VW. Recommendations for fluorine-18 production. Appl. Radiat. Isot. 1991; 42:749–762.

Kaneko S, Ishiwata K, Hatano K, Omura H, Ito K, Senda M. Enzymatic synthesis of no-carrier-added 6-[18F]fluoro-l-dopa with β^2-tyrosinase. Appl. Radiat. Isot. 1999; 50:1025–1032. [PubMed: 10391715]

Kienzle GJ, Reischl G, Machulla HJ. Electrochemical radiofluorination. 3. Direct labeling of phenylalanine derivatives with [18F]fluoride after anodic oxidation. J. Label. Compd. Radiopharm. 2005; 48:259–273.

Lee C, Yang W, Parr RG. Development of the Colle–Salvetti correlation-energy formula into a functional of the electron density. Phys. Rev. B: Condens. Matter Mater. Phys. 1988; 37:785–789.

Lee E, Hooker JM, Ritter T. Nickel-mediated oxidative fluorination for PET with aqueous [18F]fluoride. J. Am. Chem. Soc. 2012; 134:17456–17458. [PubMed: 23061667]

Lee E, Kamlet AS, Powers DC, Neumann CN, Boursalian GB, Furuya T, Choi DC, Hooker JM, Ritter T. A fluoride-derived electrophilic late-stage fluorination reagent for PET imaging. Science (Wash., DC, U. S). 2011; 334:639–642.

Lemaire C, Damhaut P, Plenevaux A, Comar D. Enantioselective synthesis of 6-[fluorine-18]-fluoro-l-dopa from no-carrier-added fluorine-18-fluoride. J. Nucl. Med. 1994; 35:1996–2002. [PubMed: 7989984]

Marten B, Kim K, Cortis C, Friesner RA, Murphy RB, Ringnalda MN, Sitkoff D, Honig B. A new model for calculation of solvation free energies: correction of self-consistent reaction field continuum dielectric theory for short range hydrogen-bonding effects. J. Phys. Chem. 1996; 100:11775–11788.

Namavari M, Bishop A, Satyamurthy N, Bida G, Barrio JR. Regioselective radiofluorodestannylation with fluorine-18 and [18F] acetyl hypofluorite: a high yield synthesis of 6-[18F]fluoro-l-dopa. Appl. Radiat. Isot. 1992; 43:989–996.

Noel M, Suryanarayanan V, Chellammal S. A review of recent developments in the selective electrochemical fluorination of organic compounds. J. Fluorine Chem. 1997; 83:31–40.

Nozaki T, Tanaka Y. Preparation of fluorine-18 labeled aryl fluorides. Int. J. Appl. Radiat. Isot. 1967; 18:111–119.

Reischl G, Kienzle GJ, Machulla HJ. Electrochemical radiofluorination: labeling of benzene with [18F]fluoride by nucleophilic substitution. J. Radioanal. Nucl. Chem. 2002; 254:409–411.

Reischl G, Kienzle GJ, Machulla HJ. Electrochemical radiofluorination. Part 2. Anodic monofluorination of substituted benzenes using [18F]fluoride. Appl. Radiat. Isot. 2003; 58:679–683. [PubMed: 12798377]

Rozhkov IN. Radical cation mechanism of the anodic fluorination of organic compounds. Russ. Chem. Rev. 1976; 45:615–629.

Sadeghi S, Liang V, Cheung S, Woo S, Wu C, Ly J, Deng Y, Eddings M, van Dam RM. Reusable electrochemical cell for rapid separation of [18F]fluoride from [18O]water for flow-through synthesis of 18F-labeled tracers. Appl. Radiat. Isot. 2013; 75:85–94. [PubMed: 23474380]

Shiue CY, Watanabe M, Wolf AP, Fowler JS, Salvadori P. Application of the nucleophilic substitution reaction to the synthesis of no-carrier-added fluorobenzene-18F and other fluorine-18-labeled aryl fluorides. J. Label. Compd. Radiopharm. 1984; 21:533–547.

Tredwell M, Gouverneur V. 18F labeling of arenes. Angew. Chem. Int. Ed. Engl. 2012; 51:11426–11437. [PubMed: 23086547]

HIGHLIGHTS

- Electrochemical nucleophilic synthesis of di-*tert*-butyl-(4-[^{18}F]fluoro-1,2-phenylene)-dicarbonate.

- Nucleophilic radiofluorination of the aromatic moiety with a radiochemical conversion of over 10%.

- 8.9 ± 1.6% decay corrected radiochemical yield of radiochemically pure product.

- The maximum specific activity value was 43 GBq/mmol.

- A tertiary-butyl group was used as an effective leaving and directing group for radiofluorination.
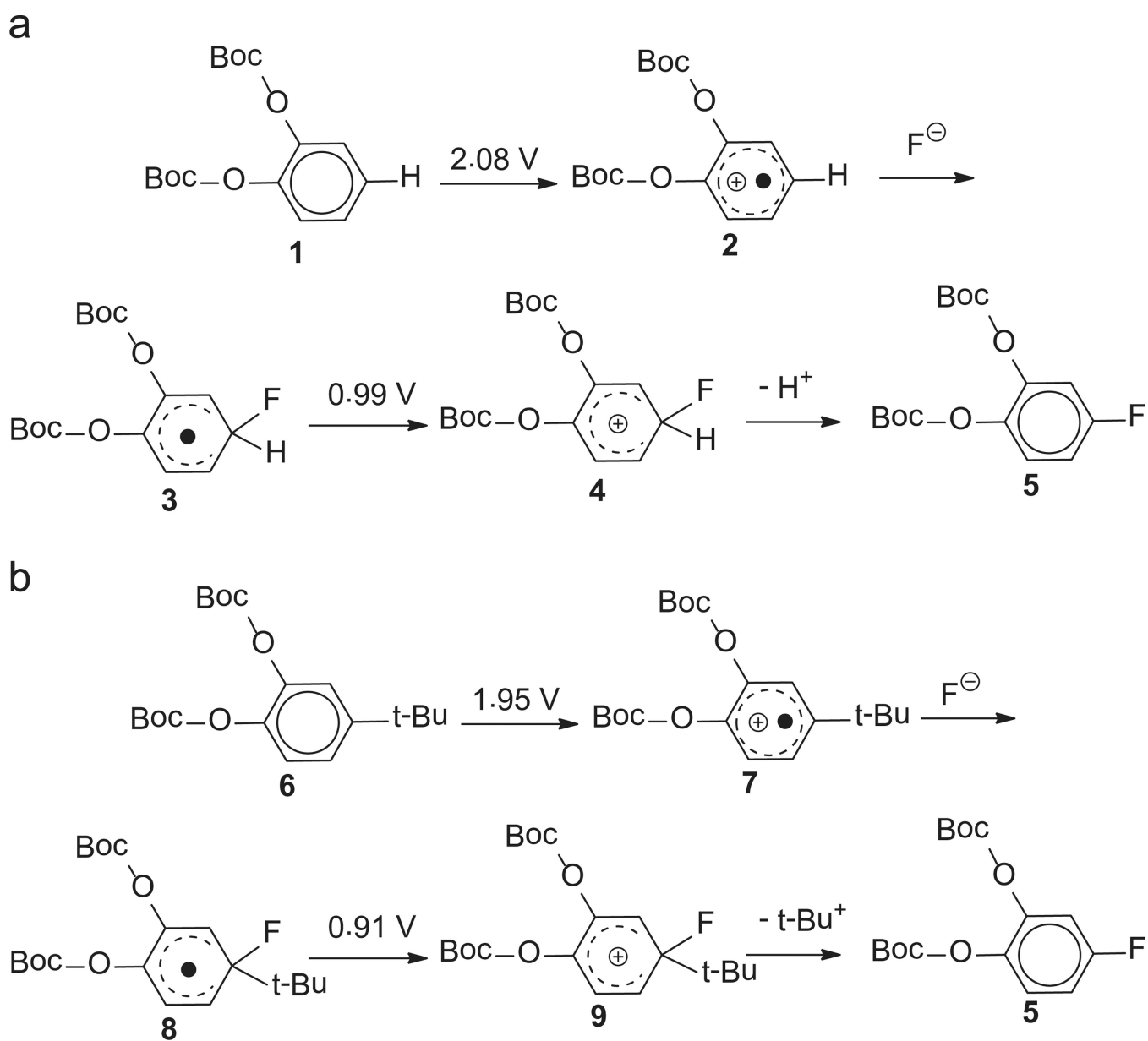
Fig. 1.
Calculated redox potentials for reactions of (a) di-*tert*-butyl-(1,2-phenylene)-dicarbonate **1** and (b) di-*tert*-butyl-(4-(*tert*-butyl)-1,2-phenylene)-dicarbonate **6**, all potential values were referred to normal hydrogen electrode (NHE).
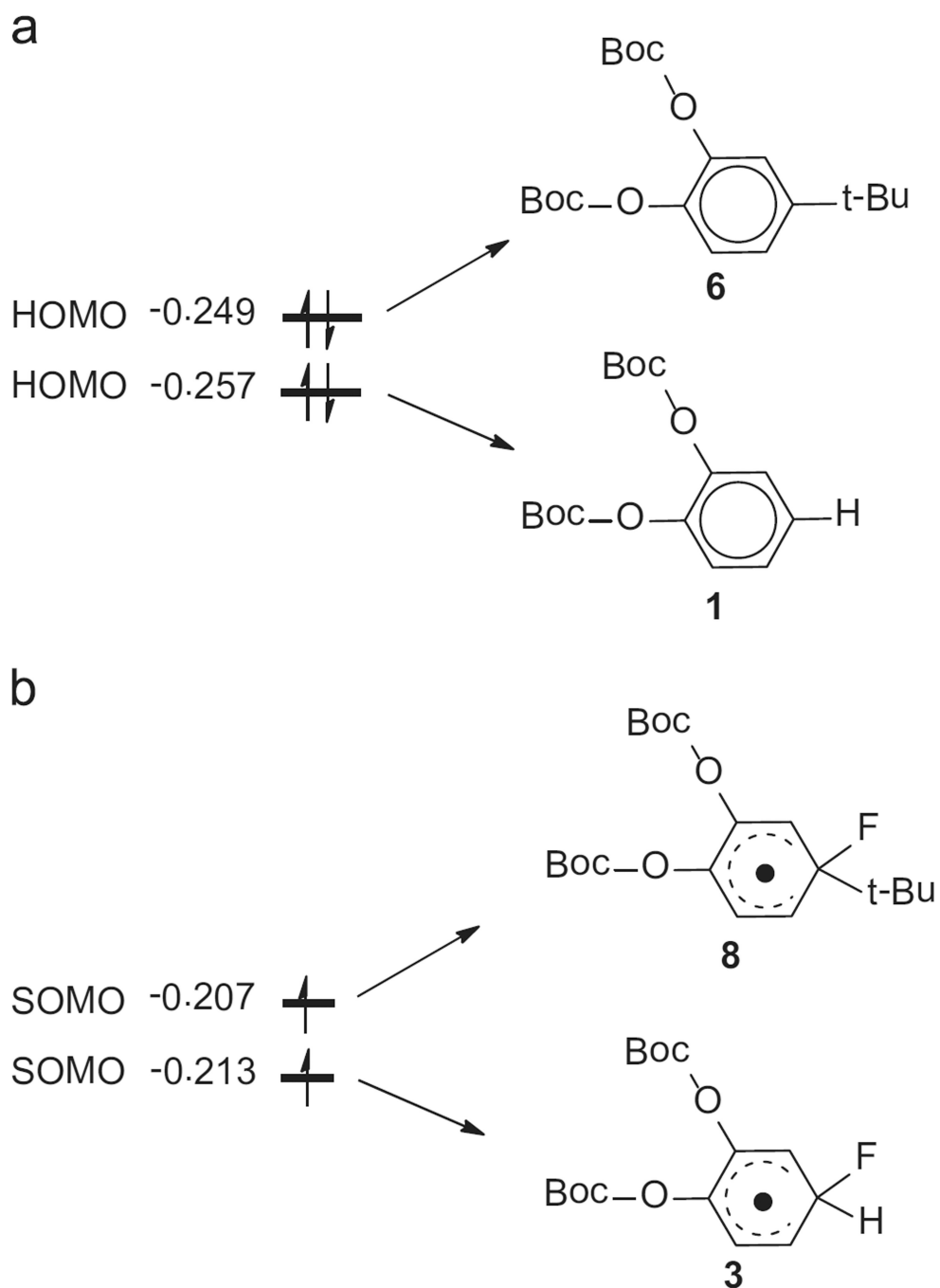
Fig. 2.
(a) HOMOs of di-*tert*-butyl-(4-(*tert*-butyl)-1,2-phenylene)-dicarbonate **6** and di-*tert*-butyl-(1,2-phenylene)-dicarbonate **1** and (b) SOMOs of fluorinated radicals from compounds **1** and **6**, the unit for orbital energyis a.u.
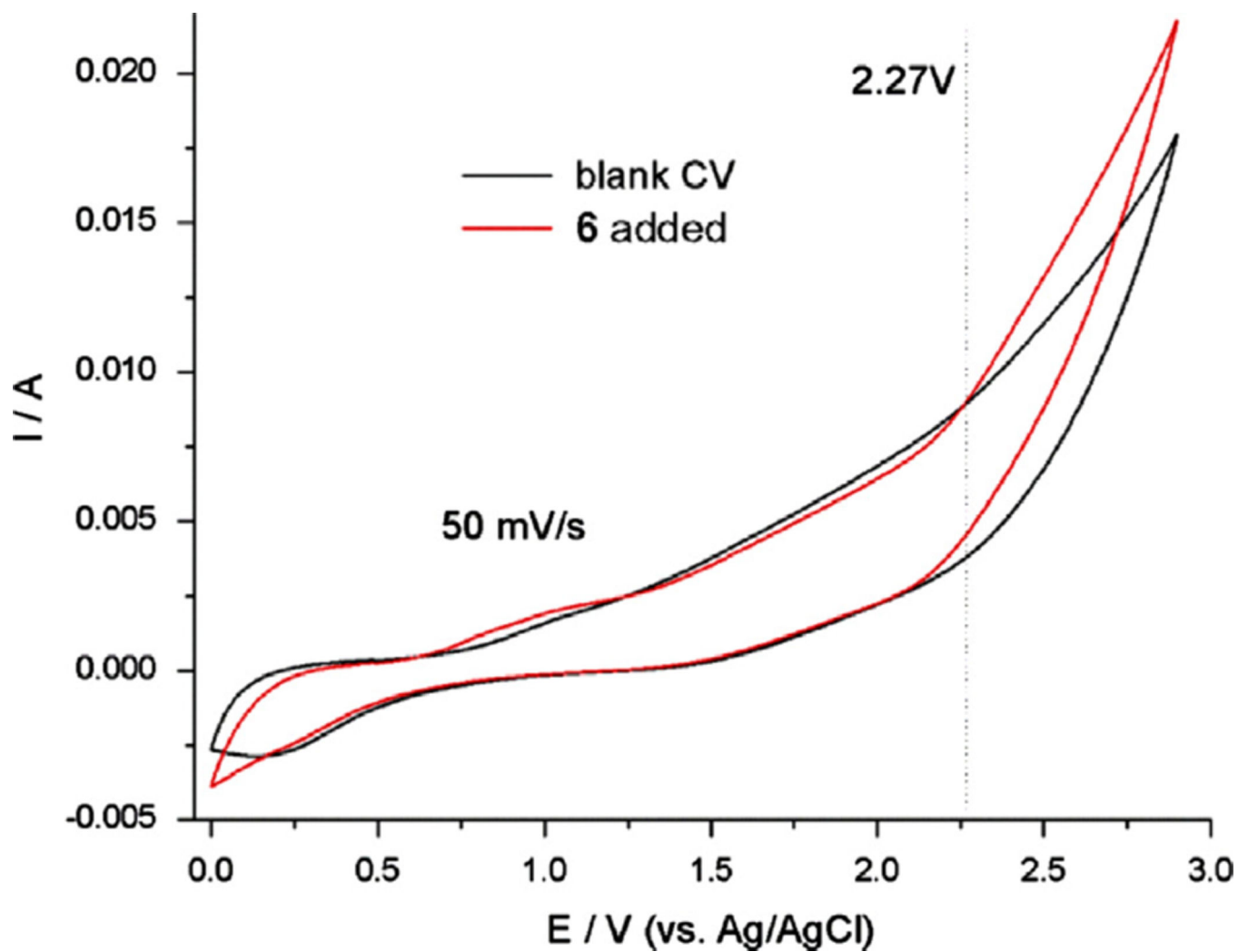
Fig. 3.
Current–potential curves in acetonitrile solution with 0.005 M **6** and 0.05 M Et$_3$N · 3HF.
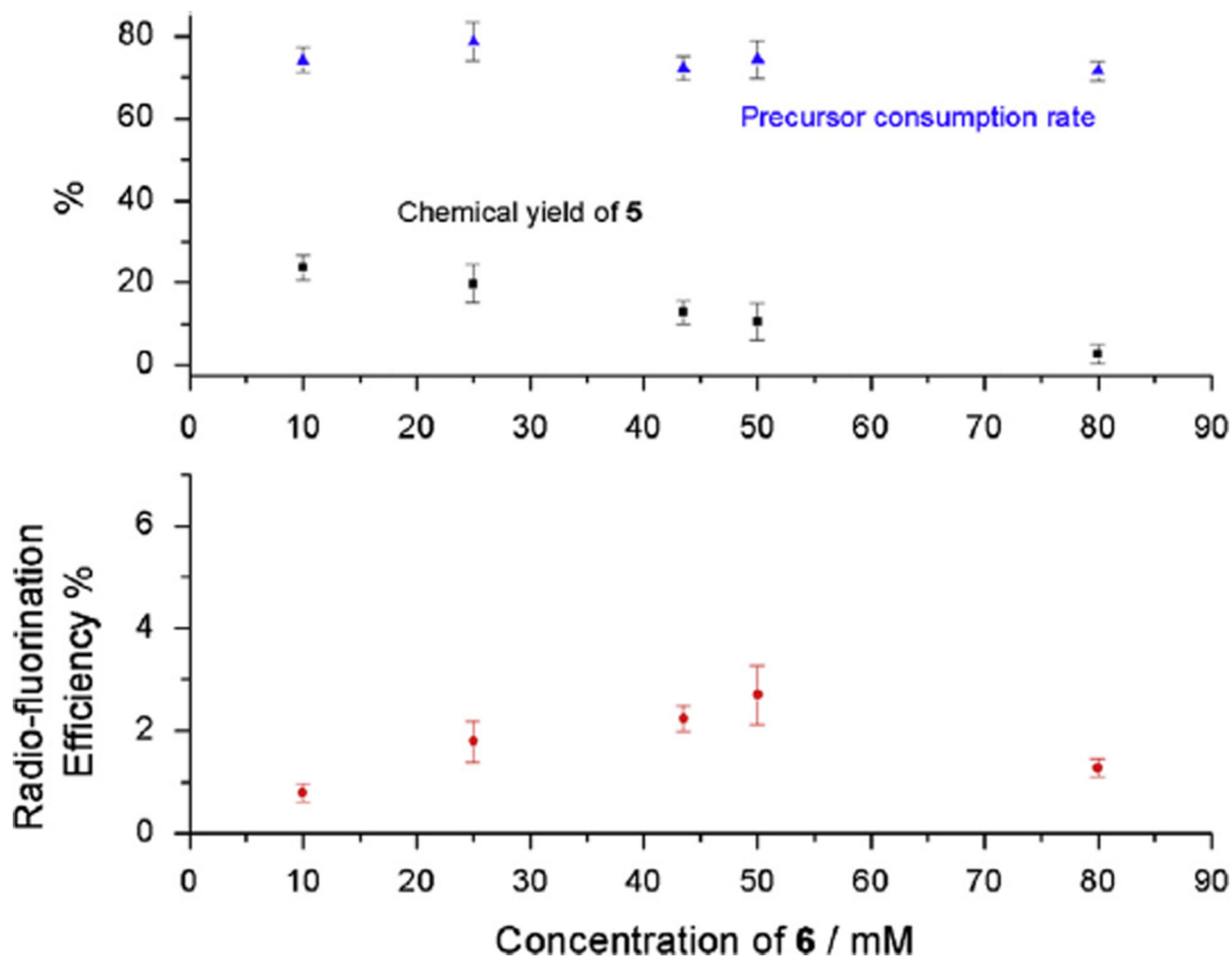
Fig. 4.
Results of electrochemical radiofluorination of different concentrations of precursor
molecule **6** in MeCN containing 0.05 M Et$_3$N · 3HF at 25 °C, in the absence of other
electrolytes
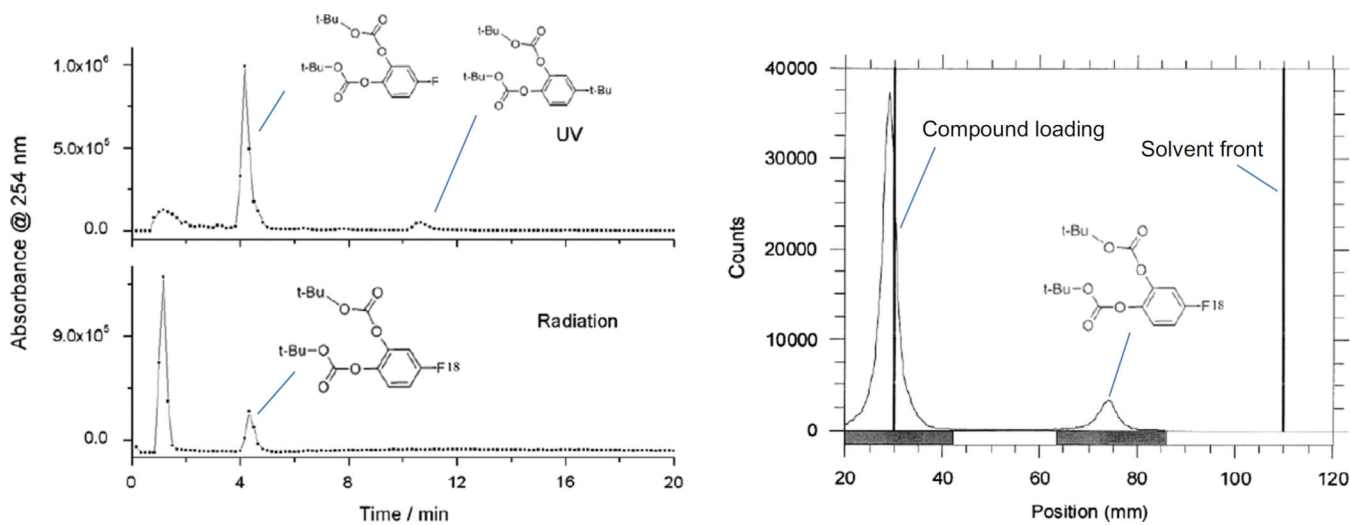
Fig. 5.
Analytical HPLC (left) and TLC (right) profiles of products of radiofluorination of **6** (0.1 M) in 0.033 M of $Et_3N \cdot 3HF$, with 0.05 M of NBu_4PF_6 as the supporting electrolyte in MeCN at 0 °C.
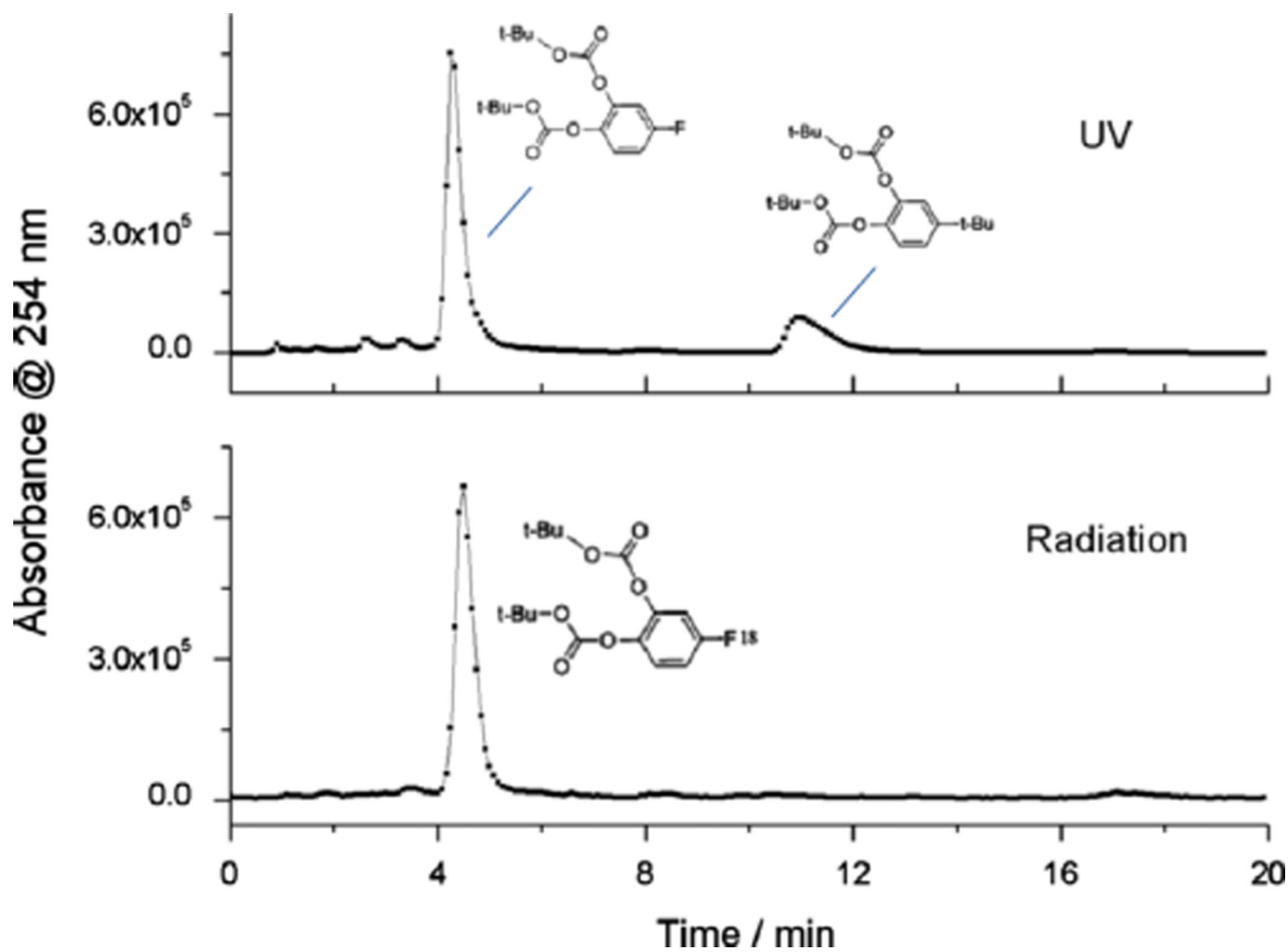
Fig. 6.
Analytical HPLC profiles of purified products of radiofluorination of **6** (0.1 M) in 0.033 M of $Et_3N \cdot 3HF$, with 0.05 M of NBu_4PF_6 as the supporting electrolyte in MeCN at 0 °C.
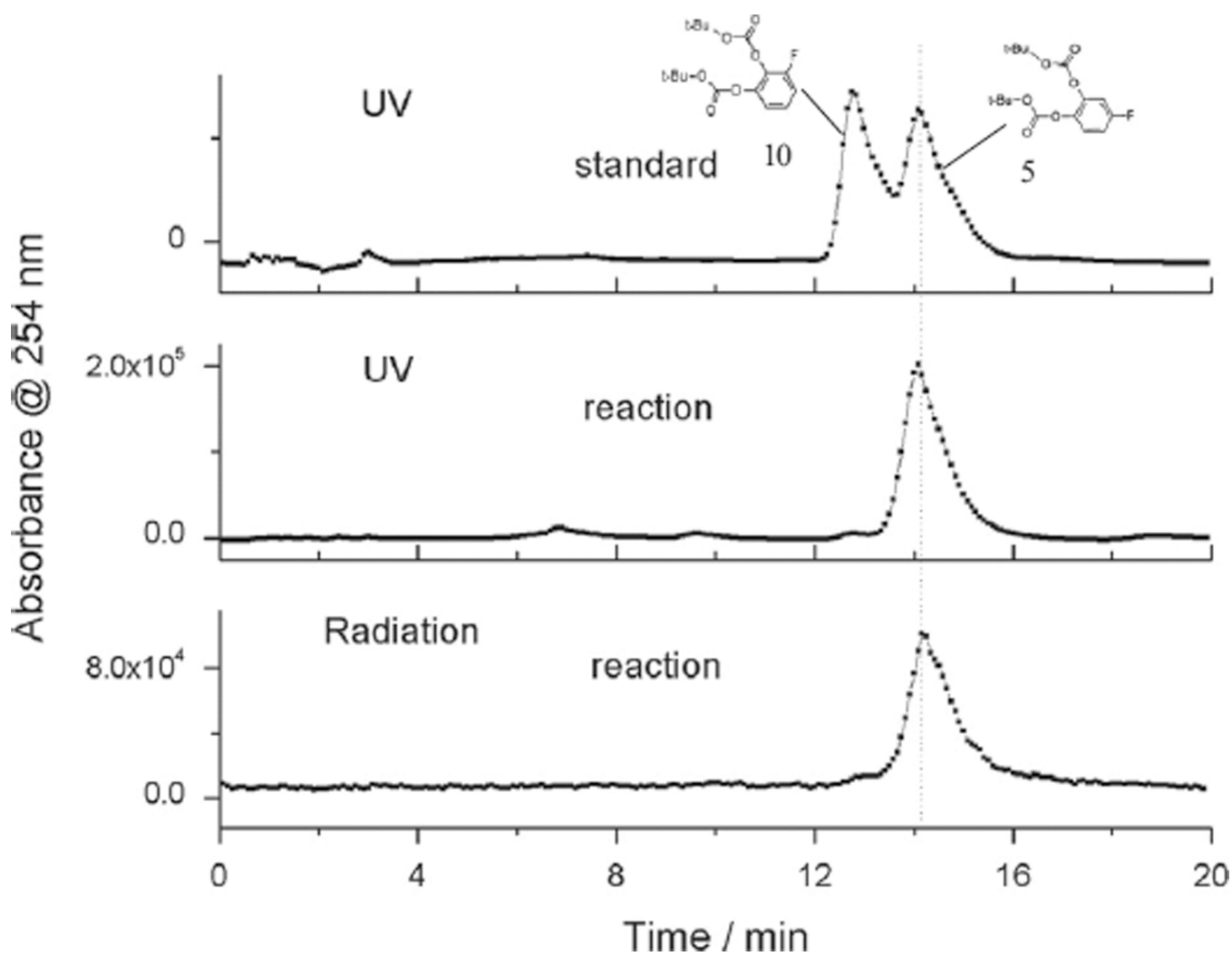
Fig. 7.
Analytical HPLC profile of standard di-*tert*-butyl-(3-fluoro-1,2-phenylene)-dicarbonate **10** and di-*tert*-butyl-(4-fluoro-1,2-phenylene)-dicarbonate **5** (top graph) and products of radiofluorination of **6** (0.05 M), with 0.033 M $Et_3N \cdot 3HF$ and 0.05 M NBu_4PF_6 at 0 °C (middle and bottom graphs); HPLC mobile phase: 60% methanol in water, flow rate: 2.0 mL min^{-1}.

Table 1

Radiofluorination efficiency of fluorination of di-*tert*-butyl-(4-(tert-butyl)-1,2-phenylene)-dicarbonate 6.

Row	Concentration of precursor (mM)	Concentration of Et$_3$N · 3HF (mM)	Concentration of supporting electrolyte (mM)		Reaction temperature (°C)	Radio-fluorination efficiency (%), ($n = 4$)
			NBu$_4$ClO$_4$	NBu$_4$PF$_6$		
1	10	50	0	0	25	0.8 ± 0.2
2	25	50	0	0	25	1.8 ± 0.4
3	43.5	50	0	0	25	2.2 ± 0.3
4	50	50	0	0	25	2.7 ± 0.6
5	80	50	0	0	25	1.3 ± 0.2
6	50	33	0	0	25	0.7 ± 0.1
7	50	33	50	0	25	3.9 ± 0.5
8	100	33	50	0	25	4.6 ± 0.4
9	100	33	50	0	0	8.6 ± 1.1
10	1010	33	0	50	0	10.4 ± 0.6